Available online at www.sciencedirect.com
SCIENCE DIRECT
Journal of Solid State Chemistry 179 (2006) 1650–1658
JOURNAL OF SOLID STATE CHEMISTRY
www.elsevier.com/locate/jssc

High-pressure synthesis, crystal structures, and characterization of $CdVO_{3-\delta}$ and solid solutions $CdVO_3$–$NaVO_3$

Alexei A. Belik[a,*], Eiji Takayama-Muromachi[b]

[a] International Center for Young Scientists (ICYS), National Institute for Materials Science (NIMS), 1-1 Namiki, Tsukuba, Ibaraki 305-0044, Japan
[b] Advanced Materials Laboratory (AML), National Institute for Materials Science (NIMS), 1-1 Namiki, Tsukuba, Ibaraki 305-0044, Japan

Received 18 November 2005; received in revised form 31 January 2006; accepted 15 February 2006
Available online 6 March 2006

Abstract

$CdVO_{3-\delta}$ and solid solutions of $Cd_{1-x}Na_xVO_3$ with the $GdFeO_3$-type perovskite structure were prepared using a high-pressure (6 GPa) and high-temperature technique. No significant oxygen and cation deficiency was found in $CdVO_3$. $Cd_{1-x}Na_xVO_3$ are formed in the compositional range of $0 \leqslant x \leqslant 0.2$. $CdVO_3$ and $Cd_{1-x}Na_xVO_3$ demonstrate metallic conductivity and Pauli paramagnetism between 2 and 300 K. A large electronic contribution to the specific heat ($\gamma = 13.4$ and 11.2 mJ/(mol K^2) for $CdVO_3$ and $Cd_{0.8}Na_{0.2}VO_3$, respectively) was observed at low temperatures due to the strongly correlated electrons. Crystal structures of $CdVO_3$ and $Cd_{0.8}Na_{0.2}VO_3$ were refined by X-ray powder diffraction: space group *Pnma*; $Z = 4$; $a = 5.33435(7)$ Å, $b = 7.52320(9)$ Å, and $c = 5.26394(6)$ Å for $CdVO_3$ and $a = 5.32056(9)$ Å, $b = 7.50289(13)$ Å, and $c = 5.25902(8)$ Å for $Cd_{0.8}Na_{0.2}VO_3$.

Keywords: High-pressure synthesis; $GdFeO_3$; Perovskite; Resistivity; Magnetic susceptibility; Specific heat; Crystal structures

1. Introduction

Transition-metal perovskites, ABO_3, have attracted much attention because of their interesting electronic and magnetic properties arising from narrow 3*d* bands, strong Coulomb correlations, and highly correlated *d* electrons. The $3d^1$ ($B = Ti^{3+}$ and V^{4+}) perovskites are particularly interesting because similar materials have very different electronic properties, and they do not show a complicated electronic structure [1].

$Ca_{1-x}Sr_xVO_3$, as a strongly correlated d^1-electron system, has been investigated a lot [1–9]. Transport and magnetic properties of $SrVO_3$ are typical for a conventional Fermi liquid [10,11]. $CaVO_3$ has been reported to be metallic and insulating, Pauli paramagnetic and Curie–Weiss paramagnetic. This large variation in properties of $CaVO_3$ reflects problems with the oxygen content [12]. Contradictory results on spectral, transport, and thermodynamic properties are also reported for $Ca_{1-x}Sr_xVO_3$ [1–9]. $SrVO_3$ crystallizes in a simple cubic perovskite structure [10] while $CaVO_3$ has the $GdFeO_3$-type perovskite structure (space group *Pnma*; lattice parameters $a = 5.3171$ Å, $b = 7.5418$ Å, and $c = 5.3396$ Å) [13].

In addition to the extensively studied $CaVO_3$ [13–15] and $SrVO_3$ [10,11], whose properties are usually investigated together [1–9,16,17], other oxides are known with the formula of $A^{2+}V^{4+}O_3$, e.g., $BaVO_3$ [18], $PbVO_3$ [19,20], and ambient- and high-pressure modifications of $CdVO_3$ [21,22]. The high-pressure modification of $CdVO_3$, HP-$CdVO_3$, was reported to have the $GdFeO_3$-type perovskite structure [22], but the crystal structure of HP-$CdVO_3$ has not been investigated yet. Down to 77 K, HP-$CdVO_3$ demonstrated metallic conductivity and Pauli paramagnetism similar to the stoichiometric $CaVO_3$. Note that the ambient-pressure modification of $CdVO_3$ crystallizes in space group *Pnma* with $a = 14.301$ Å, $b = 3.598$ Å, and $c = 5.204$ Å [21], and V^{4+} ions are located in VO_5 pyramids in comparison to the usual octahedral coordination of *B*-type ions in the perovskite-type structures. Despite the fact that $CaVO_3$ and HP-$CdVO_3$ are isotypic, there are no reports, to the best of our knowledge, about HP-$CdVO_3$ except for Refs. [22,23]. However, spectral, transport, and magnetic properties of HP-$CdVO_3$ and solid solutions including it as

*Corresponding author. Fax: +81 029 860 4706.
E-mail address: Alexei.BELIK@nims.go.jp (A.A. Belik).

0022-4596/$ - see front matter © 2006 Elsevier Inc. All rights reserved.
doi:10.1016/j.jssc.2006.02.018

the end member appear to be interesting in the same manner as those of $CaVO_3$.

In this work, we report on $CdVO_{3-\delta}$ and solid solutions of $Cd_{1-x}Na_xVO_3$ prepared at high pressure. Crystal structures of HP-$CdVO_3$ and $Cd_{0.8}Na_{0.2}VO_3$ were studied by X-ray powder diffraction (XRD). Basic physical properties of $CdVO_{3-\delta}$ and $Cd_{1-x}Na_xVO_3$ were investigated.

2. Experimental section

2.1. Synthesis

Samples with the nominal compositions of $Cd_{0.9}VO_3$ and $CdVO_{3-\delta}$ ($\delta = -0.1, 0.0, 0.1, 0.2, 0.5$) and solid solutions of $Cd_{1-x}Na_xVO_3$ ($0 \leqslant x \leqslant 0.4$) were prepared from stoichiometric mixtures of CdO (99.9%), V_2O_3, V_2O_5 (99.9%), and $NaVO_3$. The mixtures were placed in Au capsules and treated in a belt-type high-pressure apparatus at 6 GPa and 1273 K for 60–90 min. After heat treatment, the samples were quenched to room temperature (RT), and the pressure was slowly released. Single-phased V_2O_3 was obtained by reducing V_2O_5 in a mixture of 10% H_2 + 90% N_2 at 1073 K for 4 h. Single-phased $NaVO_3$ was synthesized in air from V_2O_5 and Na_2CO_3 (99.9%) at 803 K for 90 h with several intermediate grindings.

2.2. Scanning electron microscopy (SEM) and energy dispersive X-ray (EDX) analysis

SEM–EDX analysis was performed using a Hitachi S-4800 scanning electron microscope, equipped with an EDX spectrometer (Horiba, EMAX).

2.3. Thermal analysis

The thermal stability was examined in air on a SII Exstar 6000 (TG-DTA 6200) system. $CdVO_3$ and $Cd_{0.8}Na_{0.2}VO_3$ were heated up to 1093 and 993 K, respectively, at a heating–cooling rate of 10 K/min in Pt holders.

2.4. Physical properties measurements

Direct current (dc) magnetic susceptibilities ($\chi = \boldsymbol{M}/\boldsymbol{H}$) were measured on a Quantum Design SQUID magnetometer (MPMS XL) between 1.8 and 300 K in an applied field of 100 Oe (1 Oe = $(10^3/4\pi)$ A/m) under both zero-field-cooled (ZFC) and field-cooled (FC) conditions. Isothermal magnetization curves were recorded at 2 K in applied fields from −70 to 70 kOe. Specific heat, C_p, was recorded between 1.8 and 100 K on cooling at zero magnetic field by a pulse relaxation method using a commercial calorimeter (Quantum Design PPMS). Electrical resistivity was measured between 2 and 300 K by the conventional four probe method using a Quantum Design PPMS with the ac-gage current of 1 mA at 30 Hz.

2.5. XRD experiments and structure refinements

XRD data for phase analysis and structure refinement were collected at RT on a RIGAKU Ultima III diffractometer using Cu$K\alpha$ radiation. The measurement time was 1 s/step for phase analysis, and 10 s/step for structure-refinement data sets (a step width of 0.02°). The XRD data were analyzed by the Rietveld method with RIETAN-2000 [24]. Coefficients for analytical approximation to atomic scattering factors for Cd, Na, V, and O were taken from [25]. The split pseudo-Voigt function of Toraya [26] was used as a profile function. The background was represented by an nth-order Legendre polynomial. Isotropic atomic displacement parameters, U, with the isotropic Debye–Waller factor represented as $\exp(-8\pi^2 U \sin^2\theta/\lambda^2)$ were assigned to all the sites. The known impurities were taken into account during the refinements. For the known impurity phases, we refined only scale factors and lattice parameters, fixing their structure parameters. The mass fractions of impurities in the samples were calculated from the scale factors refined in their Rietveld analyses.

3. Results and discussion

3.1. Phase compositions of $CdVO_{3-\delta}$ and $Cd_{1-x}Na_xVO_3$

XRD showed that the samples with the nominal composition of $Cd_{0.9}VO_3$ and $CdVO_{3.1}$ contained a $GdFeO_3$-type phase and strong unidentified reflections (the strongest ones at $2\theta = 30.85°$, 31.00°, and 35.90°: phase I). This fact indicates that $CdVO_3$ does not have significant cation deficiency. The samples with the nominal composition of $CdVO_{2.5}$ and $CdVO_{2.8}$ contained a $GdFeO_3$-type phase and impurities of CdO, $CdCO_3$, and an unidentified phase II (with the strongest reflections at $2\theta = 19.20°$, 25.52°, and 33.60°). The formation of the $GdFeO_3$-type phase in $CdVO_{2.5}$ suggests that V^{3+} is oxidized to V^{4+} in the bulk of the sample due to the reduction of CdO to metal Cd on the surfaces:

$$3CdO + V_2O_3 = 2CdVO_3 + Cd \text{ (in Au)}. \quad (1)$$

When the sample with the nominal composition of $CdVO_{2.5}$ was treated at 6 GPa and a higher temperature of 1473 K, it contained only a $GdFeO_3$-type phase, VO_2, and a phase having the structure of Au with very broad reflections. The formation of VO_2 in this case clearly confirmed the following reaction:

$$2CdO + V_2O_3 = CdVO_3 + VO_2 + Cd \text{ (in Au)}. \quad (2)$$

Reactions (1) and (2) may also occur in the samples with the nominal compositions of $CdVO_{2.9}$ and $CdVO_{2.8}$ changing to some extent the oxygen content of the $GdFeO_3$-type phases and oxidizing V ions in the bulk of the samples. The surface of the pellets was usually strongly attached to Au capsules and removed with the capsules. This is why we could not detect metal Cd or Au in the bulk

of the $CdVO_{2.9}$, $CdVO_{2.8}$, and $CdVO_{2.5}$ samples treated at 1273 K.

Note that when the sample with the nominal composition of $CdVO_{2.8}$ was prepared at 1273 K using BN between the Au capsule and the sample, no $GdFeO_3$-type phase was found. This sample contained CdO and phase II. On the other hand, $CdVO_3$ could be prepared using BN between the Au capsule and the sample. These facts show the importance of Au in the formation of the $GdFeO_3$-type phases in the samples with the nominal composition of $CdVO_{3-\delta}$ with $\delta > 0$.

XRD showed that the solid solutions of $Cd_{1-x}Na_xVO_3$ are formed in the compositional range of $0 \leqslant x \leqslant 0.2$; even small amount of impurities VO_2 and $CdCO_3$ were found in these samples. These impurities correspond to the starting reagents. In the XRD patterns of the samples with $x = 0.3$ and 0.4, additional reflections of unidentified impurities were observed.

Figs. 1 and 2 display typical SEM images of polished pellets of $CdVO_3$ and $Cd_{0.8}Na_{0.2}VO_3$. The local EDX analysis showed that the Cd/V ratio in $CdVO_3$ varied between 0.99 and 1.04 with the average value of 1.00, confirming the cation stoichiometry of the obtained $CdVO_3$ sample. In $Cd_{0.8}Na_{0.2}VO_3$, the (Cd + Na)/V ratio was between 1.01 and 1.04 (the average value was 1.02), and the Cd/Na ratio between 0.22 and 0.26 (the average value was 0.24). These results confirmed the cation composition of $Cd_{0.8}Na_{0.2}VO_3$.

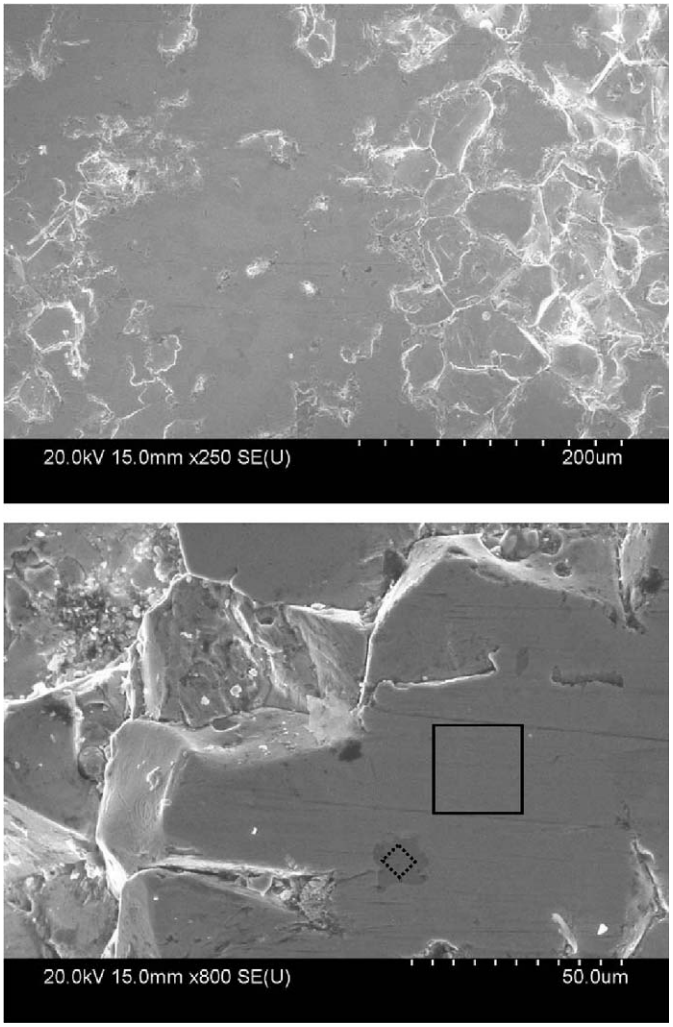

Fig. 1. Typical SEM images of the polished pellet of $CdVO_3$. The EDX results from the region shown by the solid-line rectangle are Cd/V = 1.00. The dotted-line rectangle shows the inclusion of the impurity of VO_2.

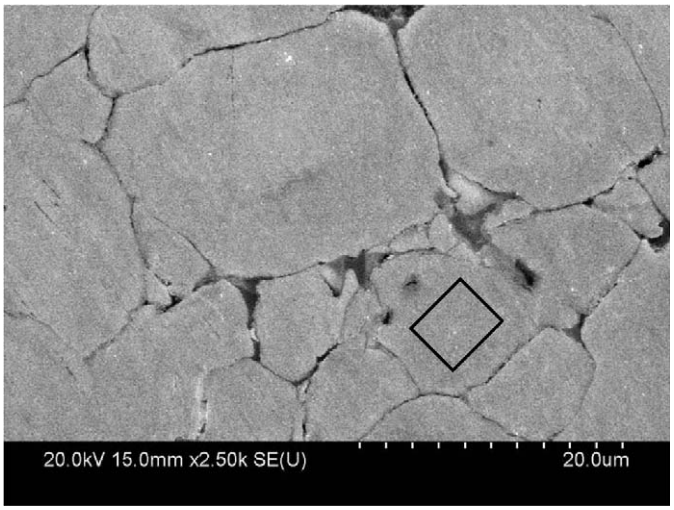

Fig. 2. Typical SEM image of the polished pellet of $Cd_{0.8}Na_{0.2}VO_3$. The EDX results from the region shown by the solid-line rectangle are (Cd + Na)/V = 1.01 and Cd/Na = 0.25.

The thermal analysis showed that $CdVO_3$ and $Cd_{0.8}Na_{0.2}VO_3$ started to be oxidized in air from about 773 and 673 K, respectively. The weight gain of $CdVO_3$ was 3.6% that is close to the theoretical value of 3.8%. The weight gain of $Cd_{0.8}Na_{0.2}VO_3$ was 3.1% that is close to the theoretical value of 3.3%. According to XRD, the final products of the oxidation were $Cd_2V_2O_7$ for $CdVO_3$ and $Cd_2V_2O_7 + NaVO_3$ for $Cd_{0.8}Na_{0.2}VO_3$. Note that for the composition of $Cd_{0.8}Na_{0.2}V^{4+}O_{2.9}$, a noticeably larger weight gain would be expected (4.2%). Therefore, the results of thermogravimetry confirmed the oxygen content of the obtained $CdVO_3$ and $Cd_{0.8}Na_{0.2}VO_3$ samples.

The lattice parameters of the $GdFeO_3$-type phase in all the samples $Cd_{0.9}VO_3$ and $CdVO_{3-\delta}$ were similar to each other (Table 1). The structure analysis of the sample with the nominal composition of $CdVO_{2.8}$ using XRD revealed no evidence for oxygen deficiency. The thermal analysis showed that the weight gain of the sample with the nominal composition of $CdVO_{2.8}$ was 3.7% that is close to that of $CdVO_3$. However, for the real composition of $CdVO_{2.8}$, the weight gain would be 5.4%. These facts support the idea that the composition of the $GdFeO_3$-type phases in the $CdVO_{3-\delta}$ samples with $\delta > 0$ was almost the same without significant oxygen deficiency.

3.2. Structure refinements of $CdVO_3$ and $Cd_{0.8}Na_{0.2}VO_3$

The XRD patterns of $CdVO_3$ and $Cd_{0.8}Na_{0.2}VO_3$ were found to be very similar to those of $GdFeO_3$-type

Table 1
Synthesis conditions, phase compositions, and lattice parameters of the $GdFeO_3$-type phases

Nominal composition	Synthesis conditions[a]	Impurities (mass fraction)[b]	Lattice parameters of the $GdFeO_3$-type phase		
$CdVO_3$	1273 K, Au	VO_2 (1%), $CdCO_3$ (<1%)	5.3344	7.5232	5.2639
$CdVO_{2.9}$	1273 K, Au	CdO (1%), $CdCO_3$ (1%)	5.3371(1)	7.5267(2)	5.2661(1)
$CdVO_{2.8}$	1273 K, Au	CdO (3%), $CdCO_3$ (2%), phase II (tr)	5.3371(1)	7.5268(2)	5.2655(1)
$CdVO_{2.8}$	1273 K, BN	CdO, phase II (st)	—	—	—
$CdVO_{2.5}$	1273 K, Au	CdO (2%), $CdCO_3$ (2%), phase II (w)	5.3344(2)	7.5229(3)	5.2622(2)
$CdVO_{2.5}$	1473 K, Au	VO_2 (13%), Au–Cd alloy (24%)	5.3358(2)	7.5249(2)	5.2629(2)
$CdVO_{3.1}$	1273 K, Au	Phase I (st)	5.3371(3)	7.5270(4)	5.2675(3)
$Cd_{0.9}VO_3$	1273 K, Au	VO_2 (2%), $CdCO_3$ (3%), phase I (st)	5.3376(3)	7.5258(4)	5.2670(3)
$Cd_{0.9}Na_{0.1}VO_3$	1273 K, Au	VO_2 (1%), $CdCO_3$ (2%)	5.3290(2)	7.5156(2)	5.2644(2)
$Cd_{0.8}Na_{0.2}VO_3$	1273 K, Au	VO_2 (1%), $CdCO_3$ (3%)	5.3206	7.5029	5.2590
$Cd_{0.7}Na_{0.3}VO_3$	1273 K, Au	Unknown	5.3160(3)	7.4987(5)	5.2599(3)
$Cd_{0.6}Na_{0.4}VO_3$	1273 K, Au	Unknown	5.2963(5)	7.5507(7)	5.2839(5)

[a]Synthesis temperature and a material surrounding the sample.
[b]tr: traces, w: weak reflections, st: strong reflections.

compounds. Therefore, for initial fractional coordinates in Rietveld analysis of $CdVO_3$ and $Cd_{0.8}Na_{0.2}VO_3$, we used those of $CaVO_3$ with space group *Pnma* [13].

The refinement of occupancy, g, of the Cd site in $CdVO_3$ resulted in $g(Cd) = 1.005(4)$. The refinement of the g value for the Cd/Na site in $Cd_{0.8}Na_{0.2}VO_3$ when only Cd was included resulted in $g(Cd) = 0.843(4)$. However, for the virtual atom $VA = 0.8Cd + 0.2Na$, $g(VA) = 1.001(4)$. Therefore, the structural data confirmed that a part of Cd was replaced by Na in $Cd_{0.8}Na_{0.2}VO_3$.

Table 2 gives experimental and refinement conditions, lattice parameters, R factors, and so forth. Final fractional coordinates and U parameters for $CdVO_3$ and $Cd_{0.8}Na_{0.2}VO_3$ are listed in Table 3, and selected bond lengths, l, and angles, ϕ, calculated with ORFFE [27] in Table 4. Fig. 3 displays observed, calculated, and different XRD patterns.

To obtain information on formal oxidation states of Cd and V, we calculated the bond valence sums, BVS [28], of the Cd and V sites in $CdVO_3$ from the Cd–O and V–O bond lengths. The resulting BVS values were 2.08 for Cd and 4.03 for V (Table 4). These BVS values support the oxidation states of +2 and +4 for Cd and V, respectively. The V–O bond lengths of $Cd_{0.8}Na_{0.2}VO_3$ were slightly shorter than those of $CdVO_3$ in agreement with the presence of V^{5+} in $Cd_{0.8}Na_{0.2}VO_3$.

Table 2
Conditions of the diffraction experiments and parts of refinement results for $CdVO_3$ and $Cd_{0.8}Na_{0.2}VO_3$

	$CdVO_3$	$Cd_{0.8}Na_{0.2}VO_3$
2θ range; step (deg)	18–148.4; 0.02	15–140; 0.02
Number of data points	6521	6251
Space group	*Pnma* (No. 62)	*Pnma* (No. 62)
Z	4	4
Lattice parameters:		
a (Å)	5.33435(7)	5.32056(9)
b (Å)	7.52320(9)	7.50289(13)
c (Å)	5.26394(6)	5.25902(8)
V (Å^3)	211.249(5)	209.938(6)
Number of Bragg reflections	232	216
Number of some variables[a]		
Background; Profiles	8; 7	10; 7
Structure (x, y, z, U)	11	10
R_{wp} (%); R_p (%)	8.83; 6.54	9.89; 7.76
R_B (%); R_F (%)	3.18; 1.88	5.24; 2.94
$S = R_{wp}/R_e$	1.67	1.87

[a]Other variables include zero shifts, scale factors, and lattice parameters.

3.3. Physical properties

$CdVO_3$ and $Cd_{0.8}Na_{0.2}VO_3$ showed metallic-like resistivity in the whole temperature range. That is, the resistivity decreased almost linearly with decreasing temperature (Fig. 4). The resistivity at 300 K (ρ_{300}) was about 0.4 Ω cm in $CdVO_3$ and 0.7 Ω cm in $Cd_{0.8}Na_{0.2}VO_3$. These values are much larger than those of typical metals, such as single crystals of $SrVO_3$ [5], but comparable with the reported values of polycrystalline samples of $SrVO_3$ ($\rho_{300} \approx 0.4$ Ω cm [10]), $CaVO_3$ ($\rho_{300} \approx 35$ Ω cm [13]), and HP-$CdVO_3$ ($\rho_{300} \approx 1$ Ω cm [22]). This is attributed to the porosity of polycrystalline samples, effects of grain boundaries, and specific distribution of impurities, for example, in grain boundaries. The pellets of $CdVO_3$ and especially $Cd_{0.8}Na_{0.2}VO_3$ were rather porous (Figs. 1 and 2). This fact can explain the large absolute values of resistivity of $CdVO_3$ and $Cd_{0.8}Na_{0.2}VO_3$. Even the absolute values of resistivity of polycrystalline samples may differ from those of single-crystals samples, the qualitative temperature dependence of resistivity of polycrystalline samples reflects the intrinsic properties. Note that the samples with the nominal compositions of $CdVO_{2.9}$ and $CdVO_{2.8}$ had $\rho_{300} \approx 0.0025$ and 0.0058 Ω cm, respectively, probably due to the better contacts between grains.

$CdVO_3$ and $Cd_{0.8}Na_{0.2}VO_3$ exhibited Pauli paramagnetic behavior of magnetic susceptibility. That is, magnetic susceptibilities were almost constant in a wide temperature

Table 3
Structure parameters for $CdVO_3$ and $Cd_{0.8}Na_{0.2}VO_3$[a]

Site[b]	Wyckoff position	x	y	z	10^2U (Å^2)
Cd	4*c*	0.03536(10)	0.25	−0.0072(2)	0.89(2)
Cd/Na[c]		0.03288(18)	0.25	−0.0058(4)	0.53(3)
V	4*b*	0	0	0.5	0.61(3)
		0	0	0.5	0.57(4)
O1	4*c*	0.4762(10)	0.25	0.0882(10)	0.8(2)
		0.4774(15)	0.25	0.0792(16)	1.0(3)
O2	8*d*	0.2884(9)	0.0439(6)	0.7075(8)	0.84(13)
		0.2928(14)	0.0391(9)	0.7074(13)	= U (O1)

[a]The first (x, y, z, and U) line of each site is for $CdVO_3$, and the second one for $Cd_{0.8}Na_{0.2}VO_3$.
[b]Occupancies of all the sites are unity.
[c]Cd/Na: g(Cd) = 0.8 and g(Na) = 0.2.

Table 4
Bond lengths, l (Å), angles, ϕ (deg), and bond valence sums, BVS [28],[a] in $CdVO_3$ and $Cd_{0.8}Na_{0.2}VO_3$

$CdVO_3$		$Cd_{0.8}Na_{0.2}VO_3$	
Bonds	l	Bonds	l
Cd–O1	2.228(6)	Cd/Na–O1	2.263(9)
Cd–O2 (× 2)	2.291(4)	Cd/Na–O2 (× 2)	2.294(6)
Cd–O1a	2.405(5)	Cd/Na–O1a	2.407(8)
Cd–O2a (× 2)	2.546(5)	Cd/Na–O2a (× 2)	2.587(8)
Cd–O2b (× 2)	2.655(5)	Cd/Na–O2b (× 2)	2.612(8)
Cd–O1b	3.025(6)	Cd/Na–O1b	2.989(8)
Cd–O1c	3.074(6)	Cd/Na–O1c	3.030(9)
BVS(Cd) with $R_0(Cd^{2+})$	2.08	BVS(Cd/Na) with R_0 (Cd^{2+})	2.05
V–O2 (× 2)	1.916(5)	V–O2 (× 2)	1.916(7)
V–O2a (× 2)	1.937(5)	V–O2a (× 2)	1.924(7)
V–O1 (× 2)	1.941(2)	V–O1 (× 2)	1.925(2)
BVS(V) with $R_0(V^{4+})$	4.03	BVS(V) with $R_0(V^{4+})$	4.14
Angles	ϕ	Angles	ϕ
O1–V–O1	180	O1–V–O1	180
O2–V–O2 (× 2)	180	O2–V–O2 (× 2)	180
O1–V–O2 (× 2)	88.8(1)	O1–V–O2 (× 2)	88.6(1)
O1–V–O2 (× 2)	90.8(1)	O1–V–O2 (× 2)	90.6(1)
O1–V–O2 (× 2)	91.2(1)	O1–V–O2 (× 2)	91.4(1)
O1–V–O2 (× 2)	89.2(1)	O1–V–O2 (× 2)	89.4(1)
O2–V–O2 (× 2)	89.2(1)	O2–V–O2 (× 2)	89.3(1)
O2–V–O2 (× 2)	90.8(1)	O2–V–O2 (× 2)	90.7(1)
V–O1–V	151.3(1)	V–O1–V	154.0(1)
V–O2–V (× 2)	153.1(1)	V–O2–V (× 2)	153.9(1)

[a]BVS = $\sum v_i$, $v_i = \exp[(R_0 - l_i)/B]$, $B = 0.37$, $R_0(Cd^{2+}) = 1.904$, and $R_0(V^{4+}) = 1.784$.

range with an upturn at low temperatures due to the presence of paramagnetic impurities or defects (Fig. 5). Almost no difference was found between the curves measured under the ZFC and FC conditions.

The $\chi(T)$ curves could be fit with the following equation [5]:

$$\chi(T) = \chi_0 + C_{imp}/(T - \theta_{imp}) + \alpha T^2, \quad (3)$$

where χ_0 is the temperature-independent term including the diamagnetic and Pauli paramagnetic contributions, C_{imp} is the impurity Curie constant, and θ_{imp} is the impurity Weiss constant. The αT^2 term is considered to originate from the higher-order temperature-dependent term in the Pauli paramagnetism that is neglected in the zero-order approximation. This term reflects the shape of the density of states at the Fermi level. The fit to Eq. (3) in the whole temperature ranges resulted in $\chi_0 = 2.945(5) \times 10^{-4}$ cm^3/mol, $C_{imp} = 4.63(8) \times 10^{-4}$ cm^3 K/mol, $\theta_{imp} = -0.01(4)$ K, and $\alpha = 3.76(11) \times 10^{-10}$ cm^3/(K^2 mol) for $CdVO_3$ and $\chi_0 = 2.968(7) \times 10^{-4}$ cm^3/V^{4+}-mol, $C_{imp} = 9.62(11) \times 10^{-4}$ cm^3 K/V^{4+}-mol, $\theta_{imp} = -0.22(3)$ K, and $\alpha = 2.3(2) \times$

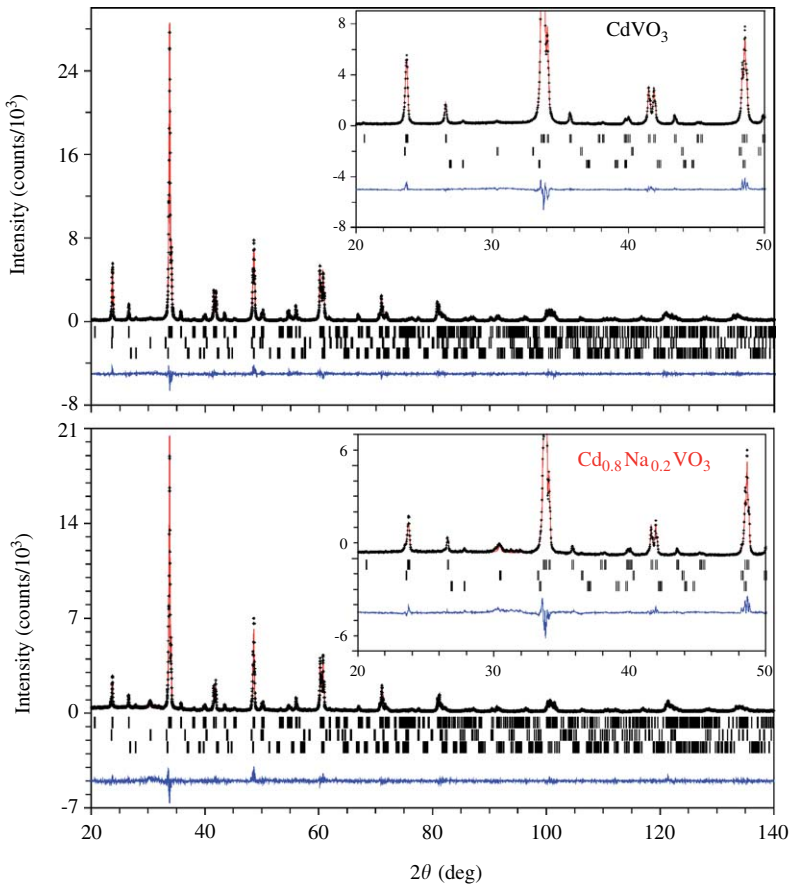

Fig. 3. Observed (crosses) and calculated (solid line) XRD patterns for $CdVO_3$ and $Cd_{0.8}Na_{0.2}VO_3$. The difference pattern is shown at the bottom. Bragg reflections are indicated by tick marks for the $GdFeO_3$-type phase (upper), $CdCO_3$ (middle), and VO_2 (lower). Insets show the enlarged fragments.

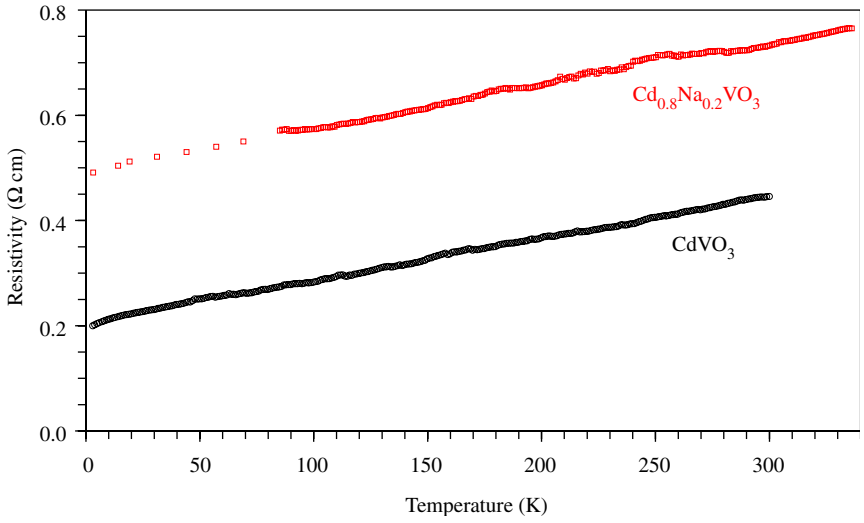

Fig. 4. Temperature dependence of the resistivity of $CdVO_3$ (circles) and $Cd_{0.8}Na_{0.2}VO_3$ (squares) measured at 1 mA.

10^{-10} cm^3/(K^2V^{4+}-mol) for $Cd_{0.8}Na_{0.2}VO_3$. The χ_0 values of $CdVO_3$ and $Cd_{0.8}Na_{0.2}VO_3$ were close to those of $CaVO_3$ and $SrVO_3$ [5,13], taking into account the fact that the diamagnetic contribution is usually one order of magnitude smaller than the obtained χ_0 values. From the C_{imp} values, we can estimate that only 0.12% and 0.26% of the V sites have

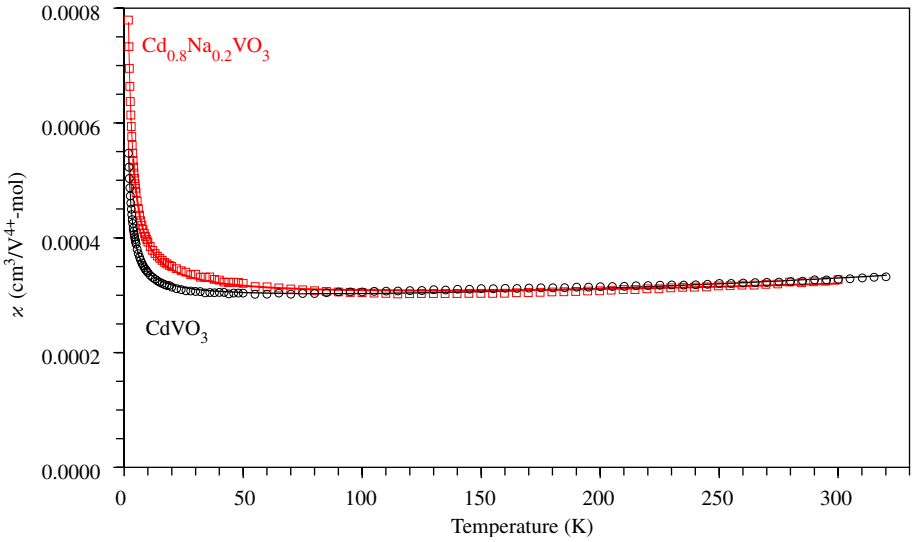

Fig. 5. Temperature dependence of the magnetic susceptibilities of $CdVO_3$ (circles) and $Cd_{0.8}Na_{0.2}VO_3$ (squares) measured at 100 Oe. The solid lines are the fits to Eq. (3) with the parameters given in the text.

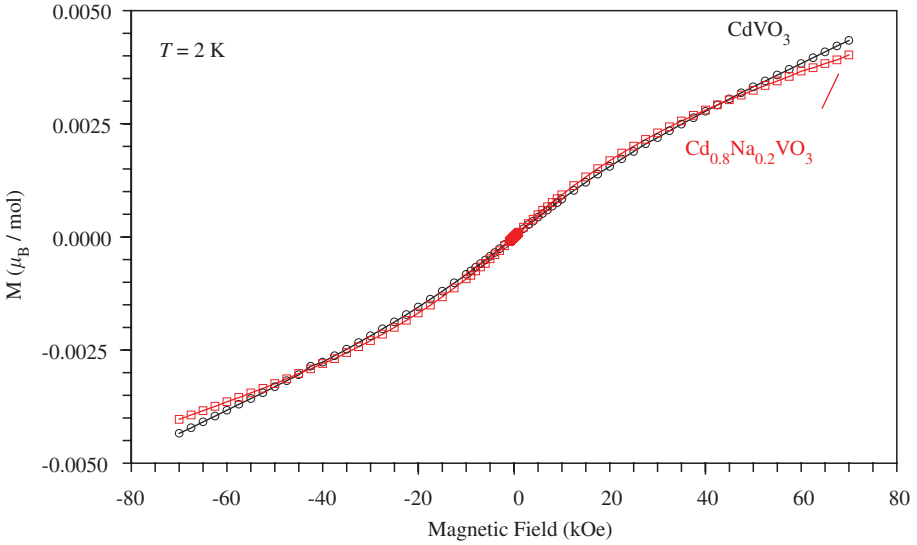

Fig. 6. The isothermal magnetization curves, M versus H, at $T = 2$ K for $CdVO_3$ (circles) and $Cd_{0.8}Na_{0.2}VO_3$ (squares).

the $S = 1/2$ local moment in $CdVO_3$ and $Cd_{0.8}Na_{0.2}VO_3$, respectively. The α values of $CdVO_3$ and $Cd_{0.8}Na_{0.2}VO_3$ were very small and close to those of single crystals of $CaVO_3$ and $SrVO_3$ [5], suggesting that the deviation from a temperature-independent Pauli paramagnetism is also very small.

The isothermal magnetization curves of $CdVO_3$ and $Cd_{0.8}Na_{0.2}VO_3$ at 2 K showed no hysteresis and reached only about 0.004 μ_B/mol at 7 T (Fig. 6). Almost the same value of magnetization was observed at 5 K and 5 T in $CaVO_3$ (0.003 μ_B/mol [13]) and $SrVO_3$ (0.002 μ_B/mol [5]). This fact indicates that only paramagnetic moments contribute to the total magnetization.

We also observed the electronic contribution to the specific heat at low temperatures in $CdVO_3$ and $Cd_{0.8}Na_{0.2}VO_3$ as can be seen from the C_p/T versus T^2 plots (Fig. 7b). The specific heat between 1.8 and 10 K could be fit by the equation

$$C_p = \gamma T + \beta_1 T^3 + \beta_2 T^5, \quad (4)$$

where the first term is ascribed to the electronic contribution with $\gamma = \frac{1}{3}\pi^2 k_B^2 N(0)$ (where $N(0)$ is the electronic density of states at the Fermi level and k_B is Boltzmann's constant), and the second and third terms describe the lattice contribution. The specific heat and magnetic susceptibility data showed no evidence for a magnetic phase transition in $CdVO_3$ and $Cd_{0.8}Na_{0.2}VO_3$. The γ values were 13.4(1) mJ/(mol K^2) in $CdVO_3$ and 11.2(1) mJ/(mol K^2) in $Cd_{0.8}Na_{0.2}VO_3$. These values are close to those of single crystals of $CaVO_3$ (9.25 mJ/(mol K^2)) and $SrVO_3$ (8.18 mJ/(mol K^2)) with strongly correlated electrons [5]. For example, in the less correlated sodium metal, $\gamma \approx 1$ mJ/(mol K^2). The values of β_1 gave the Debye

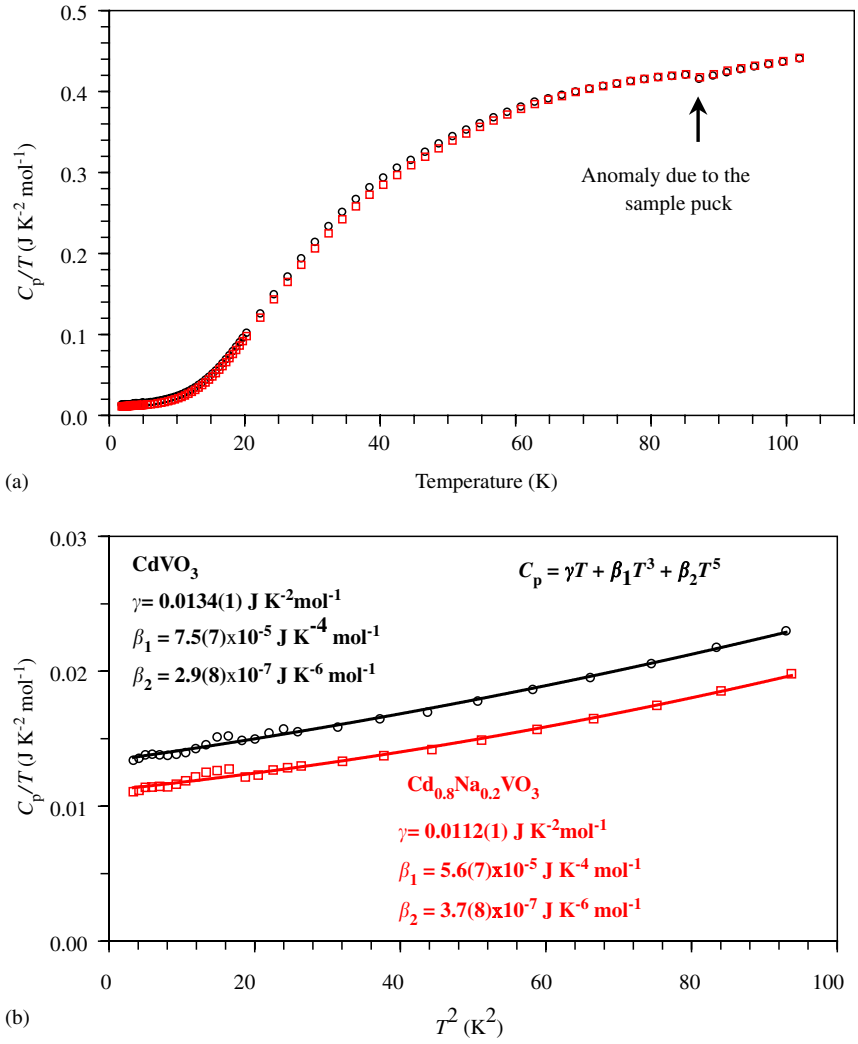

Fig. 7. (a) Total specific heat divided by temperature, C_p/T, plotted against T for $CdVO_3$ (circles) and $Cd_{0.8}Na_{0.2}VO_3$ (squares). (b) The C_p/T versus T^2 curves for $CdVO_3$ and $Cd_{0.8}Na_{0.2}VO_3$ (symbols). The solid lines are the fits to Eq. (4) with the parameters given on the figure.

temperature, $\Theta_D = (234\,Nk_B/\beta_1)^{1/3}$ (N is Avogadro's number), of 296 K for $CdVO_3$ and 326 K for $Cd_{0.8}Na_{0.2}VO_3$ comparable to the Debye temperature of $CaVO_3$ ($\Theta_D \approx 368$ K) and $SrVO_3$ ($\Theta_D \approx 322$ K) [5].

In conclusion, we have investigated the crystal structures and basic physical properties of $CdVO_3$ and $Cd_{0.8}Na_{0.2}VO_3$. Both compounds have the $GdFeO_3$-type perovskite structure and demonstrate the metallic-like resistivity and Pauli paramagnetism between 1.8 and 300 K. The properties of $CdVO_3$ and $Cd_{0.8}Na_{0.2}VO_3$ are very similar to those of $CaVO_3$ and $SrVO_3$. Investigation of a carrier-doping metal–insulator transition in solid solutions of $CdVO_3$–YVO_3 is in progress, and the results will be reported shortly.

Acknowledgments

ICYS is supported by Special Coordination Funds for Promoting Science and Technology from MEXT, Japan. We thank Dr. H. Gao of NIMS for her assistance with the SEM–EDX analysis.

References

[1] A. Sekiyama, H. Fujiwara, S. Imada, S. Suga, H. Eisaki, S.I. Uchida, K. Takegahara, H. Harima, Y. Saitoh, I.A. Nekrasov, G. Keller, D.E. Kondakov, A.V. Kozhevnikov, T. Pruschke, K. Held, D. Vollhardt, V.I. Anisimov, Phys. Rev. Lett. 93 (2004) 156402.
[2] M.J. Rozenberg, I.H. Inoue, H. Makino, F. Iga, Y. Nishihara, Phys. Rev. Lett. 76 (1996) 4781.
[3] I.H. Inoue, I. Hase, Y. Aiura, A. Fujimori, Y. Haruyama, T. Maruyama, Y. Nishihara, Phys. Rev. Lett. 74 (1995) 2539.
[4] A. Fujimori, I. Hase, H. Namatame, Y. Fujishima, Y. Tokura, H. Eesaki, S. Uchida, K. Takegahara, F.M.F. Degroot, Phys. Rev. Lett. 69 (1992) 1796.
[5] I.H. Inoue, O. Goto, H. Makino, N.E. Hussey, M. Ishikawa, Phys. Rev. B 58 (1998) 4372.
[6] H. Makino, I.H. Inoue, M.J. Rozenberg, I. Hase, K. Aiura, S. Onari, Phys. Rev. B 58 (1998) 4384.
[7] K. Morikawa, T. Mizokawa, K. Kobayashi, A. Fujimori, H. Eisaki, S. Uchida, F. Iga, Y. Nishihara, Phys. Rev. B 52 (1995) 13711.
[8] Y. Aiura, F. Iga, Y. Nishihara, H. Ohnuki, H. Kato, Phys. Rev. B 47 (1993) 6732.
[9] J. Garcia-Jaca, J.L. Mesa, M. Insausti, J.I.R. Larramendi, M.I. Arriortua, T. Rojo, Mater. Res. Bull. 34 (1999) 289.

[10] Y.C. Lan, X.L. Chen, A. He, J. Alloy. Compd. 354 (2003) 95.
[11] T. Yoshida, K. Tanaka, H. Yagi, A. Ino, H. Eisaki, A. Fujimori, Z.X. Shen, Phys. Rev. Lett. 95 (2005) 146404.
[12] H.F. Pen, M. Abbate, A. Fuijmori, Y. Tokura, H. Eisaki, S. Uchida, G.A. Sawatzky, Phys. Rev. B 59 (1999) 7422 and references therein.
[13] H. Falcón, J.A. Alonso, M.T. Casais, M.J. Martínez-Lope, J. Sánchez-Benítez, J. Solid State Chem. 177 (2004) 3099 and references therein.
[14] H.D. Zhou, J.B. Goodenough, Phys. Rev. B 69 (2004) 245118.
[15] I.H. Inoue, C. Bergemann, I. Hase, S.R. Julian, Phys. Rev. Lett. 88 (2002) 236403.
[16] I.A. Nekrasov, G. Keller, D.E. Kondakov, A.V. Kozhevnikov, Th. Pruschke, K. Held, D. Vollhardt, V.I. Anisimov, Phys. Rev. B 72 (2005) 155106.
[17] A. Liebsch, Phys. Rev. Lett. 90 (2003) 096401.
[18] G. Liu, J.E. Greedan, J. Solid State Chem. 110 (1994) 274.
[19] R.V. Shpanchenko, V.V. Chernaya, A.A. Tsirlin, P.S. Chizhov, D.E. Sklovsky, E.V. Antipov, E.P. Khlybov, V. Pomjakushin, A.M. Balagurov, J.E. Medvedeva, E.E. Kaul, C. Geibel, Chem. Mater. 16 (2004) 3267.
[20] A.A. Belik, M. Azuma, T. Saito, Y. Shimakawa, M. Takano, Chem. Mater. 17 (2005) 269.
[21] M. Onoda, N. Nishiguchi, J. Phys.: Condens. Matter 11 (1999) 749.
[22] B.L. Chamberland, P.S. Danielson, J. Solid State Chem. 10 (1974) 249.
[23] T.V. Dyachkova, N.I. Kadyrova, D.G. Kellerman, Y.G. Zainulin, Russ. J. Inorg. Chem. 37 (1992) 1374 (translated from Z. Neorgan. Khimii 37 (1992) 2663).
[24] F. Izumi, T. Ikeda, Mater. Sci. Forum 321–324 (2000) 198.
[25] A.J.C. Wilson, E. Prince, (Eds.), International Tables for Crystallography, vol. C, second ed., Kluwer, Dordrecht, The Netherlands, 1999. pp. 572–574.
[26] H. Toraya, J. Appl. Crystallogr. 23 (1990) 485.
[27] W.R. Busing, K.O. Martin, H.A. Levy, Report ORNL-TM-306, Oak Ridge National Laboratory, Tennessee, 1964.
[28] R.E. Brese, M. O'Keeffe, Acta Crystallogr. B 47 (1991) 192.